Dual heart-phase cardiac DTI using Local-look STEAM

Christian Torben Stoeck[1], Nicolas Toussaint[2], Peter Boesiger[1], and Sebastian Kozerke[1,2]
[1]*Institute for Biomedical Engineering, University and ETH Zurich, Zurich, Switzerland,* [2]*Imaging Sciences, King's College London, London, United Kingdom*

Introduction: To understand the mechanism of cardiac contraction, it is essential to investigate the myocardial morphology on a microscopic level. Up to date most studies were performed ex-vivo using histological analyses of the heart [1]. Diffusion weighted MRI of moving organs has considerably evolved over the recent past and now provides a window to investigate myocardial fiber architecture in-vivo. By analyzing strain- and the diffusion-tensors Dou et al. [2] showed, that fiber shortening and fiber shear do contribute only little to myocardial thickening, while sheet shear, sheet extension and shear normal thickening play a major role. In Chen et al. [3] excised rat hearts were fixated either in systole or diastole. Using diffusion tensor imaging a transmural change of helix angle by 10° to 30° between diastole and peak systole were found. Furthermore a significant reduction in magnitude of the sheet angle from diastole to peak systole was detected.

In this work we present an analysis of myocardial fiber architecture in humans at peak systole and diastole.

Materials and Methods: Imaging was performed on a 1.5T Philips clinical MRI system equipped with a 32 channel cardiac receiver array and a gradient system allowing a maximal gradient strength of 40mT/m at a slew rate of 200mT/m/ms per channel. Cardiac DTI data was acquired using a diffusion weighted STEAM sequence [4]. Imaging parameter were as follows: in plane resolution: 2×2mm^2, FOV: 230×105mm^2, slice thickness: 8mm, TE 20ms, 60% partial Fourier sampling. Diffusion encoding was performed along 15directions with a b-value of 500s/mm^2 and 9 averages per direction. The duration of the diffusion encoding gradients was 3ms. Each direction was acquired in a separate breathhold with a duration of 18 R-R intervals each. To guarantee same breath hold level a respiratory navigator with a gating window of 5mm was placed on the right hemidiaphragm. The regular FID crushers were removed from the sequence and replaced by the diffusion encoding gradients. Field-of-view reduction (local-look) was implemented by applying the first slice-selective excitation pulse in phase encoding direction (Figure 1), while the second and third pulse remained in slice encoding direction. Systolic and diastolic rest periods were used as imaging window. The exact timing was determined based on high temporal resolution cine images along short axis and long axis views. Slices of the diffusion weighted acquisitions were manually planed in short axis view and their positions were adjusted for the difference in ventricular length in systole and diastole. Three to five slices along the LV were acquired for both cardiac phases. A B0 map was acquired covering the LV in order to perform image based shimming. Two 3D whole-heart acquisitions were performed covering the entire LV during the systolic and diastolic rest periods. In post-processing all DWIs were co-registered and tensors were estimated for each slice. Subsequently each slice was registered to its corresponding 3D whole heart volume and a 3D tensor interpolation was performed as described by Toussaint et al. [4]. Transmural changes in helix angle (angle between first eigenvector and the transmural plane) as well as the sheet normal angle (angle between third eigenvector and the transmural plane) were calculated on interpolated tensor fields and myocardial fiber path lines were reconstructed.

Results: Figure 2 shows the transmural change of helix angle in the basal (a), equatorial (b) and apical (c) regions in systole (blue) and diastole (red). The sheet normal angle is shown for the same three regions in Figure 2 (d-f). The transmural change of helix angle was linearly fitted and the resulting slope defined as transmural change rate of the helix angle. Averaged over the entire LV the fitted helix angle change rate was -0.97 °/% transmural depth in systole while it was found to be -0.61 °/% transmural depth in diastole. The range of helix angles increased by 31° during systole when averaged over the entire LV. The magnitude of the mid-mural sheet angle was 20° lower in systole compared to diastole when averaged over the LV presenting a larger range of sheet normal angles. Figure 3 shows 3D fiber reconstructions of the entire LV in systole and diastole. Color coding corresponds to the helix angle.

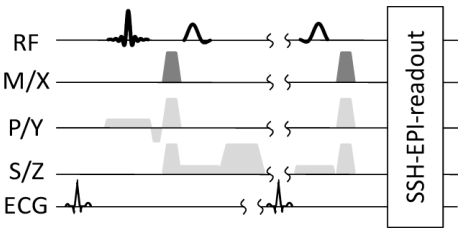

Figure 1 Schematic of the local-look STEAM sequence with diffusion encoding gradients and a single-shot EPI readout.

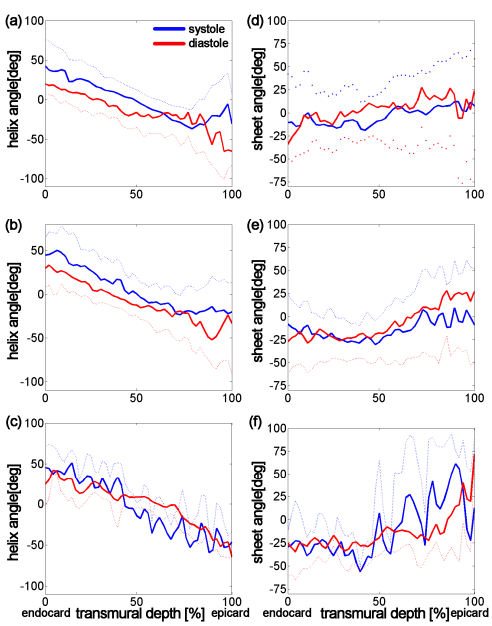

Figure 2 shows the analysis of the myocardial fiber and sheet architecture for the basal (top row), equatorial (center row) and apical (bottom row) region. The transmural helix angle distribution is shown in (a-c) as well as the transmural sheet angle distribution (d-f). Blue lines correspond to systolic and red lines to diastolic data. The dotted line represents one standard deviation across the volume of interest.

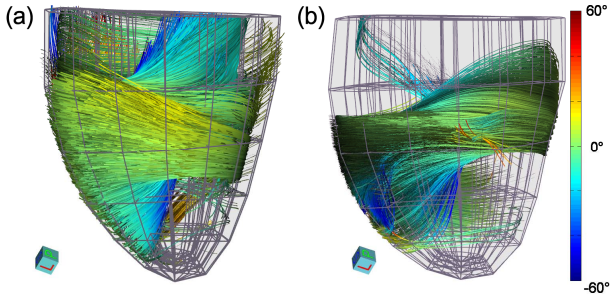

Figure 3 shows a 3D whole heart fiber reconstruction in systole (a) and diastole (b). The color coding represents helix angle.

Discussion and Conclusion: We have presented initial results and the feasibility of dual phase human cardiac DTI in-vivo. Although showing a large standard deviation in apical regions helix angle do compare well with previous results [4]. The greater standard deviation in the apex may be related to the lower density sampling and reduced image quality in apical regions. A reorientation of fiber sheets towards a lower magnitude in sheet angle as reported by Chen et al. [3] could be confirmed in this study. Remaining deviations in magnitude might be addressed to the significantly lower image resolution in-vivo as compared to what can be achieved ex-vivo.

References: [1] Anderson et al. Clin. Anat. 2009; [2] Dou et al. MRM 2003; [3] Chen et al. AJP 2005 ; [4] Tseng et al. MRM 1999 ; [5] Toussaint N. et al. MICCAI 2010;